A&A 466, 1211–1217 (2007)
DOI: 10.1051/0004-6361:20066040

Astronomy & Astrophysics

Study of the primary cosmic ray mass composition using gamma rays

V. Kopenkin[1,2] and Y. Fujimoto[2]

[1] Skobeltsyn Institute of Nuclear Physics, Moscow State University, Moscow, Russia
e-mail: vvk20032004@yahoo.com
[2] Advanced Research Institute for Science and Engineering, Waseda University, Tokyo, Japan

Received 14 July 2006 / Accepted 14 January 2007

ABSTRACT

Context. The gamma rays detected by passive balloon-borne emulsion chambers in the stratosphere give additional information on primary cosmic ray composition and allow indirect testing of the conclusions based on the study of the primary particle tracks.
Aims. We search for a consistent view of the balloon experiments with traditional calorimeter-type emulsion conducted at various atmospheric depths in the stratosphere. Using analytical calculation, we test two models of primary composition based on experimental information given by these experiments.
Methods. We analyze original experimental data relevant for the inquiry, consider the risk of empirical and methodical bias, and test the consistency of data sets with different hypotheses.
Results. It is shown that observed experimental data on gamma rays are in agreement with the atmospheric origin of their production. We notice that observed experimental signals in the energy region above 10 TeV can be an indication of an increase of heavy primaries. However, quantitative analysis does not show statistically significant evidence in favor of one specific composition model.

Key words. cosmic rays – gamma rays: theory – instrumentation: detectors – methods: data analysis – infrared general

1. Introduction

During last 30 years there have been several direct experiments (JACEE, Sanriku, MUBEE, RUNJOB) with traditional calorimeter-type emulsion chambers[1] to study the cosmic ray mass composition in the energy region $10^{12} \sim 10^{15}$ eV nucleon^{-1} performed at different altitudes in the stratosphere (Asakimori et al. 1998; Zatsepin et al. 1994; Apanasenko et al. 1998; Kawamura et al. 1989). Some observations reported a gradual increase in mass number with energy (Takahashi 1998; Apanasenko et al. 1998, 1999b; Shibata 1999), indicating that for energies above 100 TeV the contribution of heavy primaries becomes significant (Kawamura et al. 1989), and showing that "the flux of "all particles" consists of the nuclei mainly" (Zatsepin et al. 1994). Another observation (RUNJOB 1995–1996) suggested that "the average mass is nearly constant over the wide energy range 20−1000 TeV particle^{-1}", and reported that there are no drastic changes at higher energies (Apanasenko et al. 2001), similar to what was observed below the knee. These two sets of results lead to quite different alternatives in relation to the astrophysical problems, such as source, acceleration, and propagation mechanisms of cosmic rays (see, for instance, Kobayakawa et al. 2002; Prouza & Smida 2003). Experiments with the emulsion chambers observe protons and heavy nuclei, as well as gamma rays (*and*/*or* electrons). Traditionally, it is believed that a large part of the observed particles consist of secondary gamma rays from the decay of neutral pions produced in the atmosphere. We re-analyze the reported observation of gamma rays with the motivation to see whether all the reported experimental data are consistent with only one hypothesis, an increase of heavy primaries near the knee region of the cosmic ray spectrum.

[1] A calorimeter is an experimental apparatus that measures the energy of particles. A calorimeter-type emulsion chamber is a detector that consists of X-ray films, nuclear emulsion plates, and other light or heavy material plates. Most particles enter the calorimeter and initiate a shower, and the particles' energy is deposited in the calorimeter, collected, and measured.

2. Experimental data on gamma rays

In Table 1, we show basic general information on passive balloon-borne experiments JACEE (Takahashi 1998), Sanriku (Kawamura et al. 1989), and RUNJOB (RUNJOB collaboration 2000), which explicitly reported observation of gamma rays. Table 2 presents a brief summary of gamma ray data, and Fig. 1 shows gamma ray energy spectra. It was reported that all the relevant experiments used the same transition curves for the determination of the cascade shower energy (Apanasenko et al. 2001; Kawamura et al. 1989).

JACEE identified the first electron-positron pair tracks from a gamma ray in emulsion plates. On the basis of approximate calculations for the preliminary analysis, the JACEE experiment reported observation of 99 gamma rays in the energy region 3–30 TeV during the 1987 and 1988 long-duration flights from Australia to South America for 120–150 h (JACEE-7 and JACEE-8) at the atmospheric depth 5–5.5 g cm^{-2}. The Sanriku experiment reported that the "gamma ray is easily identified in nuclear emulsion by tracing the electron shower up to its original point" (Kawamura et al. 1989). Among 200 showers ($\Sigma E_\gamma >$ 2 TeV, zenith angle tg $\theta < 3.73$) observed by Sanriku, there were 106 showers identified as being of atmospheric gamma ray origin. JACEE and Sanriku showed consistency in their results (at 2 TeV and 1–10 TeV, respectively) in comparison with the independent experiment (Nishimura et al. 1980, 1987).

Table 1. Passive balloon-borne emulsion chamber experiments discussed in the present study.

Experiment	Years	Effective altitude g cm^{-2}	Accumulated exposure m^2 h	Chamber area m^2	Source
JACEE	1979–1996	3.3–8.	1436.	0.20–1.20	(Takahashi 1998)
Sanriku	1987	32.8	12.4	0.4	(Kawamura et al. 1989)
RUNJOB	1995–1999	10–12	575.	0.4	(RUNJOB collaboration 2000)

Table 2. Reported data on gamma rays from passive balloon-borne emulsion chamber experiments. (MFP stands for proton mean free path.)

Experiment	Years	Effective altitude g cm^{-2}	Flight hours	Chamber height (cm)	Calorimeter (MFP)	Energy range E_γ TeV	Source
JACEE	1987	5.5	150.	~15	~0.25	3–30	(Takahashi et al. 1995) (Fuki 2001)
	1988	5	120.	~12	~0.25		
Sanriku	1987	32.8	31.1	~13.7	~0.25	2–80	(Kawamura et al. 1989)
RUNJOB	1995	10–12	297.	~39	~0.18	~1–300	(RUNJOB collaboration 2000)
	1996	10–12	281.5	~21	~0.17	~0.5–90	

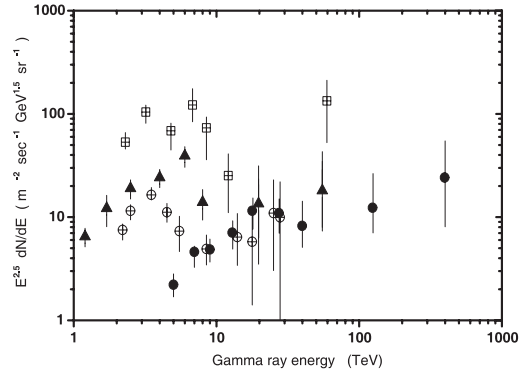

Fig. 1. Differential energy spectrum of gamma rays measured by JACEE (circles with crosses) at 5.5 g cm^{-2} (Takahashi et al. 1995), Sanriku (squares with crosses) at 32.8 g cm^{-2} (Kawamura et al. 1989), RUNJOB 1995 (triangles), and RUNJOB 1996 – IIIA (solid circles) at 10–12 g cm^{-2} (RUNJOB collaboration 2000). The vertical axis is multiplied by $E^{2.5}$. JACEE and Sanriku reported absolute gamma ray flux observed at their altitudes. The RUNJOB data show the lower bounds (see text).

RUNJOB reported the best statistics on gamma rays compared to the other two experiments. The RUNJOB 1995–1996 data constitutes 40% of the total accumulated exposure of RUNJOB (see Table 1). The identification of gamma rays in the RUNJOB experiment was made by observing "the feature of the cascade shower" (RUNJOB collaboration 2000). Tracing results obtained in RUNJOB 1995 and RUNJOB 1996 are presented in Table 3. "Wall" showers are showers with the vertex point most likely out of the chamber. NA stands for "not available". Adjacent showers (from block to block) are included in "etc.". The RUNJOB chamber consists of 4 blocks. The number of detected showers in RUNJOB 1996 is about four times that in RUNJOB 1995. This is explained by the differences in the detection conditions (RUNJOB collaboration 2000). There is an agreement of the gamma ray flux between different blocks of RUNJOB 1996. It can be seen that the fraction of gamma showers to total number of showers in RUNJOB 1995 and RUNJOB 1996 is ~40–50% . The fraction of showers identified as protons was about 20–30%, based on the same routine identification procedure. It was noted that gamma rays could be contaminated by nucleons (Apanasenko et al. 1999c). The "ratio of doubtful identification" was estimated as "not more than 7% among gamma and proton initiated cascades" (Apanasenko et al. 1999c). Due to the change in methodical procedure in one of the blocks (IVB) of RUNJOB 1996, gamma rays were removed from the sample of the analysis (RUNJOB collaboration 2000). Thus, RUNJOB 1996-IVB had smaller statistics, ~30% lower, compared to others (see Table 3).

The original gamma ray differential energy spectrum (RUNJOB collaboration 2000) was not corrected for the solid angle and the detection efficiency η. Since the effective solid angle at the top of the atmosphere can be expressed as $\Omega = \int\int_{\Omega<2\pi} \cos\theta d\Omega = \pi$, then the distribution for the atmospheric gamma rays should be $F_\gamma(\cos\theta)d\cos\theta \sim d\cos\theta$ because the gamma rays are produced in the overlying residual atmosphere, and thus have a $sec\theta$ enhancement relative to the isotropic case. In the ideal case $\eta = 1$, the maximum solid angle is $2 \times \pi$. Using these corrections, we can consider the RUNJOB gamma ray spectra presented in Fig. 1 as the lower bounds.

2.1. Proton spectrum

It was reported that the proton spectrum observed by RUNJOB and Sanriku (see Fig. 2) is consistent with JACEE within statistical errors (Apanasenko et al. 1998, 1999a, 2000, 2001). Thus, one can consider that the process of setting the magnitude of the output (or response) of a particular detector to the magnitude of the input proton flux has been done by all three experiments. Using the absolute proton flux estimate (the same for the relevant experiments), we can calculate the flux of secondary gamma rays (expected from protons) at the altitude of observation. Estimations of the secondary gamma ray flux (from heavy primaries) can be based either on analytical calculation, or model simulation, using different models.

Comparing the results of the calculation with the reported experimental data on absolute gamma ray flux, we can test the validity of our assumptions.

Table 3. Statistics on observed showers from the RUNJOB 1995 and RUNJOB 1996 campaigns (Apanasenko et al. 1999b, 2001; RUNJOB collaboration 2000).

Primary	1995 4 blocks	1996 – IIIA 1 block	1996 – IIIB 1 block	1996 – IVA 1 block	1996 – IVB 1 block	1996 4 blocks
Proton	117	100	NA	NA	NA	339
He-Fe	53	46	NA	NA	NA	152
Not identified, "wall", etc.	37	12	53	42	76	183
Gamma rays	174	226	201	186	78	691
Number of available showers	381	384	420	404	289	1497

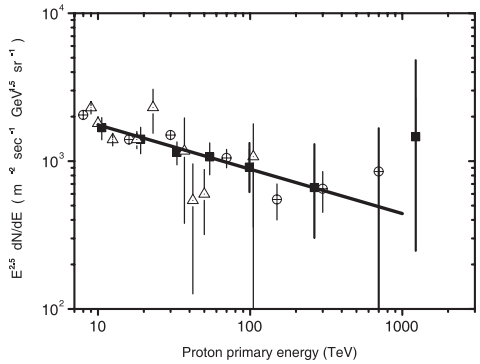

Fig. 2. Fluxes of proton components as a function of primary energy E_0 obtained by different experiments. The vertical axis is multiplied by $E_0{}^{2.5}$. Circles: the JACEE data (Asakimori et al. 1998). Triangles: the Sanriku data (Kawamura et al. 1989). Squares: the RUNJOB 1995–1996 data (Apanasenko et al. 2001). Solid line: proton spectrum suggested by RUNJOB with power-law index $\beta = 2.8$ (Apanasenko et al. 2001). The data shown here are limited to experiments using passive techniques only. For the recent compilation of the data on proton flux from the latest generation of payloads based on active (electronic) detection techniques see, for instance, Wefel et al. (2005) and Seo (2006).

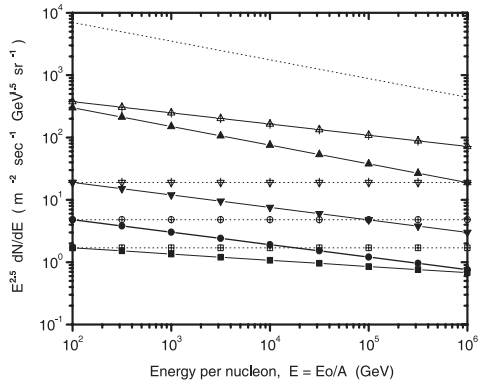

Fig. 3. The primary cosmic ray composition displayed by the energy per nucleon in the HJ model and the PR model. Protons (solid line) are assumed to be the same in the HJ model and the PR model. The HJ model is represented by dot lines with upward triangles (helium), downward triangles (CNO), circles (NeMgSi), and squares (iron). The PR model is represented by solid lines with upward triangles (helium), downward triangles (CNO), circles (NeMgSi), and squares (iron). The integral power indices of each component are (β_p:β_{He}:β_{CNO}:β_{NeMgSi}:β_{Fe} = 1.8:1.68:1.5:1.5:1.5) in the HJ model and (β_p:β_{He}:β_{CNO}:β_{NeMgSi}:β_{Fe} = 1.8:1.8:1.7:1.7:1.6) in the PR model.

2.2. Study of gamma rays

Gamma rays at balloon altitudes are from two sources: the primary gamma rays from outer space and secondary gamma rays (or atmospheric gamma rays). Basically, atmospheric gamma rays are due to neutral pions from nuclear interactions in the overlaying atmosphere. With increasing depth of the observation, one expects an increased flux of atmospheric gamma rays, and thus, the flux is proportional to the atmospheric depth at balloon altitude. The gamma ray energies observed in the balloon experiments cover ~1–100 TeV. The atmospheric gamma rays have been produced by primaries with much higher energies. Thus, from the investigation of the gamma ray intensity, one can deduce the primary spectrum in the region ~10–1000 TeV nucleon^{-1}.

Assuming that the nuclear interaction mechanism does not change with energy, and taking into account the measured primary cosmic-ray flux, it is possible to calculate the expected secondary particle flux at the particular level of observation. Analysis of the differences between proton and gamma ray spectra would indicate: change of composition, as well as methodical problems. It was shown (Berezovskaya et al. 1997) that a slow increase of proton cross sections or an increase of inelasticity does not result in changes of gamma ray energy spectrum slope in comparison with the primary proton spectrum.

2.3. The working models

We consider two models of primary composition (see Fig. 3): the heavy composition model (HJ) and the proton dominant model (PR). The absolute fluxes and power indices of different primary components were chosen on the basis of the experimental information given by JACEE (Takahashi 1998) and RUNJOB (Apanasenko et al. 2001). We assume that the power index does not change with energy for each primary component in the limited energy interval of our concern. The integral power indices of each component are chosen as (β_p:β_{He}:β_{CNO}:β_{NeMgSi}:β_{Fe} = 1.8:1.68:1.5:1.5:1.5) in the HJ model and (β_p:β_{He}:β_{CNO}:β_{NeMgSi}:β_{Fe} = 1.8:1.8:1.7:1.7:1.6) in the PR model.

For the study of gamma rays, in particular, we may use the findings from our study with the use of the mountain based X-ray emulsion chambers exposed at Mt. Chacaltaya and at the Pamirs (Kopenkin et al. 2002, 2003). Basically, the balloon-borne experiments utilize the same type of calorimeter type detector. The gamma ray production from nuclear interactions is within the validity of standard hadron theory, at least up to the interaction energy as high as ~10^{15} eV. Thus, we are able to rely on the theoretical estimation of secondary gamma rays from the primary particles with assumed energy spectra and composition. Under

the assumption of no change of nuclear interaction in the energy region up to $\sim 10^{15}$ eV nucleon^{-1}, the power index is kept the same from the primary component to the secondary. The relation between the primary flux and the secondary one can be expressed by a simple set of parameters, illustrated as follows: i) atmospheric collision of a primary nucleus of mass A, where $N_{\rm int}(A)$ – is the average number of nucleon interactions in nucleus collision with an air nucleus and $N_{\rm spec}(A)$ – the average number of spectator nucleons $N_{\rm spec}(A) = A - N_{\rm int}(A)$; ii) production of gamma rays in nucleon collision is described by the effective gamma ray multiplicity $n_{\rm eff}(\gamma)$. If we consider only the relation between gamma rays and protons (*and*/*or* nucleons), and the composition is made on an equal shower energy basis, then the inelasticity parameter can be neglected. The remaining parameter is $n_{\rm eff}(\gamma)$. The effective gamma ray multiplicity can be evaluated from our mountain chamber experiment. The assumed parameter values are: $N_{\rm int}$(He:CNO:NeMgSi:Fe) = 2:7:14:14, and $n_{\rm eff}(\gamma) = 3$.

2.4. Energy spectrum of gamma rays

The expected gamma ray spectrum at the depth t (g cm^{-2}) in the atmosphere can be estimated analytically. The primary energy spectrum of the nucleus with mass number A is expressed as $I_{\rm A}(E){\rm d}E = N_{\rm A}E^{\beta}{\rm d}E/E$, where E_0 is the primary energy and E is the energy per nucleon, i.e., $E = E_0/A$. Usually the spectra are multiplied by $E^{2.5}$, and presented in the form $E^{2.5}I_{\rm A}{\rm d}E = N_{\rm A}E^{\beta+1.5}{\rm d}E$. The atmospheric interaction can be approximated in average, as a superposition of nuclear interactions of $N_{\rm int}(A)$ participating nucleons, with the association of $N_{\rm spec}(A)$ spectator nucleons. Each nucleon collision produces $n_{\rm eff}(\gamma)$ gamma rays with energy E_γ, that is $E_\gamma = k_\gamma E/n_{\rm eff}(\gamma)$. The gamma ray spectrum at a given atmospheric depth can be obtained after summation over the contribution from every component of the primary cosmic rays and from the secondary nucleons of spectators. Within the relevant atmospheric depths, the atmospheric cascade process gives only small corrections.

3. Comparison of data

Comparison of the experimental data with the models is presented in Figs. 4–6. The results of the analytical calculation can be compared with the simulation (see Fig. 6), for instance with (Apanasenko et al. 1999c), where a computer code was developed on the basis of a well-known three-dimensional Monte Carlo simulation GEANT, and a nucleus-nucleus interaction simulation with a QGSJET generator for high energies (above ~80 GeV), and the standard GEISHA code for lower energies. Our analytical estimations show that we can reproduce experimental results obtained by JACEE and Sanriku, that is increase the heavy primaries with energy. RUNJOB 1996-IIIA agrees with RUNJOB 1995 on gamma ray flux, the gamma ray spectrum, and the ratio of observed gamma rays to the total number of observed showers. There is an agreement of the gamma ray flux between different blocks of RUNJOB 1996. RUNJOB 1995 shows an increase of the average mass number with energy that is confirmed by the observation of primary particle tracks (Apanasenko et al. 1998, 1999b; Shibata 1999), as well as by gamma rays. Thus, we show that original experimental data of RUNJOB 1995 and RUNJOB 1996 are consistent with the same hypothesis of increase of heavy primaries with energy.

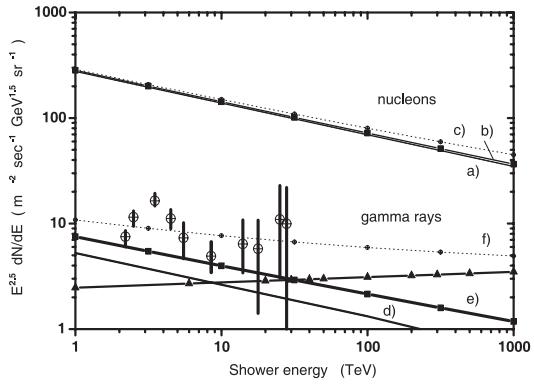

Fig. 4. Differential energy spectrum of showers measured at the altitude ~5 g cm^{-2}. Lines show the results of calculations for the expected proton flux (a), nucleon flux (in the PR model (b), and in the HJ model (c)), and gamma ray flux (from protons (d), in the PR model (e), and in the HJ model (f)) at the top of the chamber. The JACEE flux (circles) was measured at 5.5 g cm^{-2} (Takahashi et al. 1995). Solid lines with triangles show extrapolation of the EGRET data based on the power-law differential energy spectrum with exponent $\beta = 2.45$ (Ohishi et al. 2005) corrected for the altitude of observation. The x-axis shows shower energy (E_γ) of gamma rays and nucleons detected in the emulsion chamber.

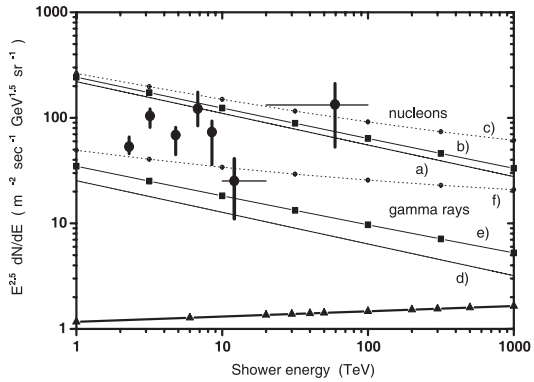

Fig. 5. Differential energy spectrum of showers measured at the altitude ~30 g cm^{-2}. Marks are same as in Figs. 3 and 4. Solid circles: the Sanriku data obtained at the effective altitude 32.8 g cm^{-2} (Kawamura et al. 1989).

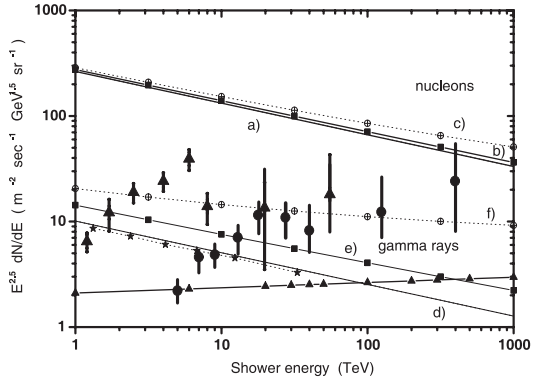

Fig. 6. Differential energy spectrum of showers measured at the altitude ~10 g cm^{-2}. Marks are same as in Figs. 3 and 4. Solid circles: the RUNJOB 1995 data (4 blocks) at the effective altitude 10–12 g cm^{-2} (RUNJOB collaboration 2000). Triangles: the RUNJOB 1996 data (one block RUNJOB 1996 – IIIa) at the effective altitude 10–12 g cm^{-2} (RUNJOB collaboration 2000). Stars and dotted lines show the Monte Carlo simulation from a previous study on the relation between the proton dominant primary composition and the expected gamma ray flux (Apanasenko et al. 1999a).

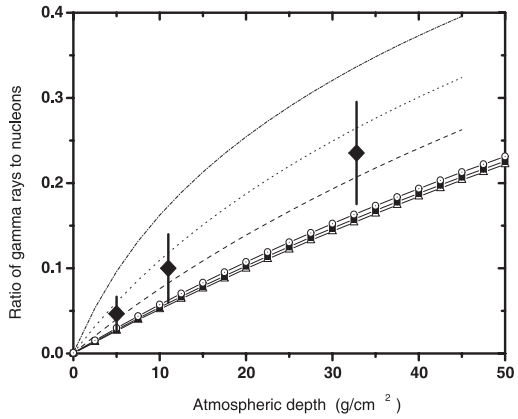

Fig. 7. Observation of the ratio of gamma rays to nucleons at the top of the chamber at different altitudes. The dashed line (1 TeV), dotted line (10 TeV), and dashed-dotted line (100 TeV) are for the HJ model. Solid lines with triangles (1 TeV), squares (10 TeV), and circles (100 TeV) are for the PR model. Experimental points (see Figs. 4–6) show estimations of the ratio of gamma rays to nucleons at 10 TeV.

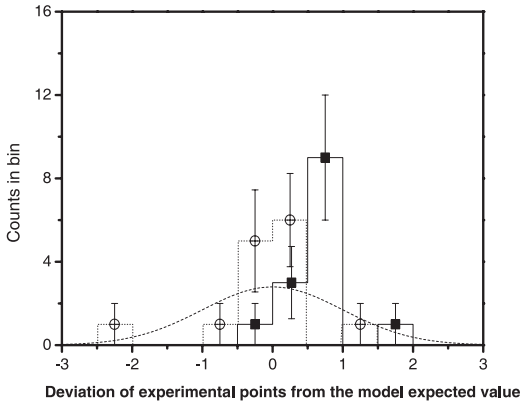

Fig. 8. The distribution of the deviation of observed values from the expectation in the energy region above 10 TeV. Solid lines and squares show deviations from the PR model, and dotted lines and circles from the HJ model. Dashed lines stand for the Gaussian distribution. Experimental estimations are based on 14 experimental points from all three experiments (Figs. 4–6).

3.1. Ratio of gamma rays to nucleons

Let us examine the ratio of gamma rays to nucleons at the top of the chamber placed at three different altitudes. Figure 7 presents an altitude variation of the observed number of gamma rays and expected number of nucleons at the top of the chamber using two models. Solid lines show the calculation for various energy thresholds (1 TeV, 10 TeV, 100 TeV). We use data from JACEE and Sanriku as they were reported and published. In the case of RUNJOB, we use our estimations of the lower bounds for secondary gamma ray flux. Since experiments were performed at three distinctly different altitudes, and there is no question of energy calibration, we can then eliminate the problem of systematic differences. The ratio of gamma rays to protons helps to deduce the primary composition. We can notice that a series of repeated measurements reveals an evident pattern, the increase of the observed gamma rays with depth of observation, in agreement with the atmospheric origin of their production. Nevertheless, given the statistical uncertainties of the 3 data points, one cannot reach statistically significant conclusions in favor of one specific composition model.

3.2. Analysis of the observed gamma ray energy spectra

Here we show a comparison of experimental data with model expectations (see Figs. 4–6).

3.2.1. Test of the cosmic gamma ray hypothesis

The atmospheric gamma ray flux observed by the emulsion chambers represents an important background to any possible signal of astrophysical origin. Before arriving at the conclusion we may consider the possibility that the excess of gamma ray flux over the expected one, based on the PR model, may be caused by cosmic gamma rays. For that purpose, we can use the results of direct galactic gamma ray measurements. JACEE estimated the upper bounds for astrophysical gamma rays. The JACEE data did not support a very hard differential spectrum $E^{-\beta}$ with an index of $\beta < 2$. The EGRET experiment (Hunter et al. 1997) in space performed direct measurements of 40 MeV–50 GeV gamma rays from the galaxy. We assume that the differential energy spectrum above 10 GeV follows a power law. Extrapolation of the EGRET spectrum to the TeV energy region with the power-law exponent $\beta = 2.45$ (Ohishi et al. 2005) is shown in Figs. 4–6. If galactic cosmic rays follow $\beta = 2.7$, then the signal would be out of the picture frame, below 1. Recent ground-based observations obtained the following spectral indices: $\beta = 2.6$ (Atkins et al. 2005) and $\beta = 2.5$ (Aharonian et al. 2001). Their estimations of the upper limits for cosmic gamma rays in the energy region ∼1–10 TeV show consistency with extrapolations from the EGRET data (Ohishi et al. 2005).

The reported astrophysical gamma ray flux and the flux of secondary gamma rays are consistent with the experimental observation of gamma rays reported by JACEE, Sanriku, and RUNJOB. If the majority of gamma rays observed at balloon altitudes were of astrophysical origin, then one would expect that the signal would decrease with increasing depth of observation, rather than increase. The hypothesis of a very high level of gamma ray flux of astrophysical origin would be also in contradiction with the Sanriku observation.

3.2.2. Comparison with two models

There are three experiments (JACEE, Sanriku, and RUNJOB) and two models (HJ and PR). It is reasonable, intuitive, and correct that the best-fitting line will be the one that minimizes the deviations in the y-direction between the experimental points and the calculated line. We can see that at high energies (>10 TeV) many experimental points are apparently above the PR model prediction. It may suggest that some additional source of gamma rays (for instance, heavy primaries) could be present. One can notice that in the same energy region, experimental points are above the HJ model curve, as well as below the curve. Based in Figs. 4–6, we estimate the deviation of experimental points from those calculated as $(y - \mu_{\rm model}/\sigma)$, where y is the experimental flux, $\mu_{\rm model}$ is the expected model flux, and σ reflects dispersions in the quantities observed. The results are shown in Fig. 8. Quantitative comparison, for instance, χ^2 or t-score, does not statistically show significant evidence in favor of either model. Therefore, the result still requires more statistics for a conclusive judgment.

3.3. Gamma ray peaks below 10 TeV

One may notice that all the concerned experiments indicate that in the energy region (<10 TeV) there are some enhancements (peaks) of observed gamma-rays over the expected secondary gamma ray flux (see Figs. 4–6. The peaks observed by JACEE, RUNJOB, and Sanriku are not necessarily of the same origin. Previous analysis of the JACEE gamma ray data indicated (Strausz 1997) that there is a monoenergetic gamma-ray peak at energy (3.5 ± 0.3 TeV), which rises 3.2σ above the flux expected from an $E^{-2.7}$ spectrum averaged over the entire 2–30 TeV energy range. There was a hypothesis (Strausz 1997) that this peak offers evidence for annihilations of super-symmetric dark matter. This observation was later rebounded by Biller & Buckley (1998) on the grounds that the upper limits cannot be used to provide evidence for a peak in the 3–4 TeV region. At lower (than JACEE) altitudes (for instance, RUNJOB, Sanriku), the same signal would be lost in the increased flux of atmospheric produced gamma rays.

The amplitude of the peaks observed by RUNJOB and Sanriku increases with the depth of observation. Such behavior itself is consistent with the atmospheric origin of their production. Considering the emulsion chamber detector, this signal is compatible with the effect of the energy threshold. One can distinguish between the minimum energy of a shower ($E_{\min}$) observed in the detector and the threshold energy of a shower, ($E_{\rm th}$). Showers with energy above ($E_{\rm th}$) are assumed to be detected with the efficiency close to 1. It is well known that if we have the power law spectrum $E^{-2.8}$, then 10% correction in energy is equivalent to ∼30% correction in intensity. Considering the low energy showers from the interval ($E_{\min}, E_{\rm th}$), the uncertainty in energy is much higher than 10%. As a result, one can expect a large fluctuation in intensity. Based on these experimental observations, we may conclude that the astrophysical nature of the peak at 3.5 TeV observed by JACEE can be verified only by future experiments performed at very high altitudes (similar to that of JACEE), or by satellite observations.

4. Heavy primary hypothesis

The JACEE and Sanriku experiments have some advantages over RUNJOB. JACEE is conducted at the very top of the atmosphere, thus reducing the effect of the atmospheric effect. In spite of the large depth of the observation, the Sanriku experiment does not suffer from a very large background of shower tracks, due to the short exposure time. The RUNJOB experiment has two objective obstacles – a large background and the not negligible effect of the atmospheric overburden effect.

The Sanriku data on gamma rays are consistent with JACEE observation of primary tracks. The JACEE experiment shows consistency between the primary particle tracks and the gamma ray signal. Our analysis of direct observation of the gamma ray signal at three different depths in the atmosphere indicates that all three experiments are consistent with the heavy primary composition model. Taking into account the reported statistics and methodical procedure, we can suggest that the actual data on primary particle tracks in RUNJOB 1995–1996 are consistent, in fact, with both hypotheses, the heavy primary and the proton dominant composition. We can conclude that the contradictions between different observations appear only at the stage of the experimental data interpretation.

4.1. Pev proton event

The RUNJOB 1995–1996 experiment reported an observation of "a single proton" with primary energy around 10^{15} eV as an indication of "the absence of a cut-off region somewhere around 100 TeV" (Apanasenko et al. 2001). Taking into account that the observational altitude in the RUNJOB experiment was 10–12 g cm^{-2}, and the arrival zenith angle of this particle was determined as $\theta \sim 64.5$ degrees, the slant depth would be around ∼30 g cm^{-2}. In fact, the particle itself could be not a primary proton, but a spectator nucleon from an interaction of a heavy primary particle with an air nucleus.

Considering an individual shower, it is impossible to determine whether it is originated by a primary proton, or by a nucleon from a heavy primary nucleus. A group of showers with the same values of the zenith and azimuthal angles could indicate the arrival of a cosmic ray family produced by a heavy primary nucleus. If secondary nucleons from heavy primaries were not taken into account (for instance, due to the change in methodical procedure), then some heavy primaries would be missing. Experiments in the stratosphere already reported observations of clear examples of such families (Perkins & Fowler 1964; Kopenkin & Fujimoto 2003). To study this topic in a particular experiment, a special new examination of the whole minimum bias event database would be required.

4.2. Mass composition and average mass

As the indicator of the composition, one can use mean values of the logarithm of mass number A (see Fig. 9). The average mass number is expressed as $\langle \ln A \rangle (E_p) = \Sigma \Delta J_m (\ln A_m)/\Sigma \Delta J_m$, where ΔJ_m is a differential intensity for the element m with mass number A_m in the energy bin $(E_p, E_{p+\Delta_p})$. The initial composition at 10^{12} eV is taken as $\langle \ln A \rangle = 1.41$ (Wiebel-Sooth et al. 1994). The JACEE data show a gradual increase in mass number at 10–1000 TeV nucleus^{-1} (Takahashi 1998). The average mass $\langle \ln A \rangle$ reported by RUNJOB 1995–1996 is "nearly constant over the wide energy range 20–1000 TeV particle^{-1}" (Apanasenko et al. 2001). This conclusion stems from the plot on the average mass against primary energy (see Fig. 9). As one can see, both models (the HJ model and the PR model) show an increase of the average mass number. If the spectra behaved as reported (Apanasenko et al. 2001), then the average mass would increase. We present data for different charge groups from RUNJOB 1995–1996 (Apanasenko et al. 2001) and JACEE (Takahashi 1998) in Table 4. Estimations for RUNJOB 1995–1996 can be made on the basis of data from (Apanasenko et al. 1998, 2001; RUNJOB collaboration 2000). JACEE data are taken from (Takahashi 1998). NA stands for "not available". It is obvious that RUNJOB does not have enough statistics to separately observe each element in the very high energy region above 100–300 TeV, and the result is quite sensitive to the size of the chosen energy bin $(E_p, E_{p+\Delta_p})$.

5. Conclusions

In summary, the following elements fit into a complete picture consistent with the hypothesis that gamma rays observed by balloons in the stratosphere are mainly secondary gamma rays from interaction with primary cosmic rays in the overlayed atmosphere:

1. abundance of gamma rays among all observed detected particles;

Table 4. Number of events for different charge groups.

Primary	140–300 TeV RUNJOB	300–500 TeV RUNJOB	>500 TeV RUNJOB	116–300 TeV JACEE	300–930 TeV JACEE	>930 TeV JACEE
Protons	2	1	1	14	3	0
Helium	3	0	0	22	7	1
C, N, O	2	0	0	12	9	1
Ne, Mg, Si	1	0	0	9	3	0
SubFe ($Z > 17$)	NA	NA	NA	9	3	2
Fe	2	1	0	NA	NA	NA

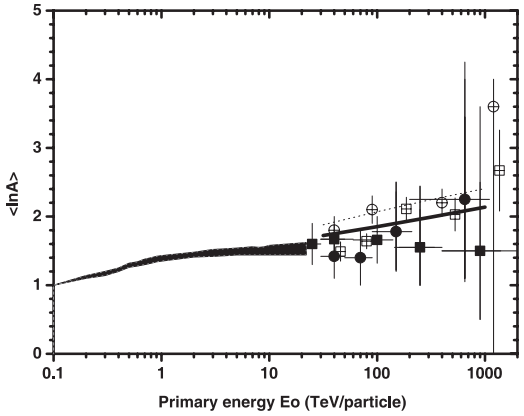

Fig. 9. Comparison of the average mass $\langle \ln A \rangle$ evaluated by different observations with estimates from the HJ model and the PR model. Open circles with crosses: the JACEE data from the first six balloon flights (Burnett et al. 1990). Open squares with crosses: the JACEE data from twelve balloon flights (Takahashi 1998). Solid circles: the RUNJOB 1995 data (Apanasenko et al. 1998, 1999b). Solid squares: the RUNJOB 1995–1996 data (Apanasenko et al. 2001). Dotted line: the HJ model, solid line: the PR model. The filled area (Apanasenko et al. 2001) corresponds to the average mass number estimated from the past direct observations.

2. increase of the ratio of gamma rays to nucleons with energy, particularly above ~10 TeV;
3. increase of the observed gamma ray flux with depth of observation, in agreement with the atmospheric origin of their production.

We noticed that observed experimental signals from all three experiments in the energy region above 10 TeV can be an indication of an increase of heavy primaries near the knee region. Nevertheless, to show quantitiative statistically significant evidence in favor of a specific composition model, more statistics are necessary. Even in the present situation of limited accuracies and large uncertainties, analysis of the observed experimental signal based on a different approach (gamma rays instead of particle tracks) provides an important test of theoretical and methodical considerations. We assume that work with original experimental materials is the basis for further theoretical models, and agree that further "mutual cross checks are quite desirable among different observers" (Kamioka et al. 1997), particularly in the treatment of those data that are still under active analysis. To refine our conclusions, in the future it will be interesting to see statistically significant results on heavy primaries from long duration balloon experiments that utilize not passive x-ray emulsion chambers, but electronic detectors.

Acknowledgements. We thank Prof. K. Kondo and Prof. S. Torii for the opportunity to work at the premises of the Advanced Research Institute for Science and Engineering, Waseda University during the preparation of this work. We express our gratitude to the late Prof. N. L. Grigorov (Skobeltsyn Institute of Nuclear Physics, Moscow State University), who honestly and courageously helped us to understand many mistakes and inconsistencies contained in a large variety of presentations. The authors wish to thank the anonymous referee for advice, valuable suggestions, and comments. V.K. would like to express his respect to colleagues and participants in the RUNJOB collaboration for the realization of the balloon experiment in the stratosphere in 1995-1999, and gives his very sincere thanks to the staff and authorities of Waseda University, Aoyama Gakuin University, Hirosaki State University, Institute for Cosmic Ray Research of Tokyo University, and the National Diet Library (Kokuritsu Kokkai Toshokan) for the opportunity to work at their facilities, and for their kindness, cooperation, and practical help.

References

Aharonian, F. A., Akhperjanian, A. G., Barrio, J. A., et al. 2001, A&A, 375, 1008
Apanasenko, A. V., et al. (RUNJOB collaboration) 1998, preprint ISAS, 37, 113
Apanasenko, A. V., et al. (RUNJOB collaboration) 1999a, Proc. 26th ICRC, Salt Lake City, 3, 163
Apanasenko, A. V., et al. (RUNJOB collaboration) 1999b, Proc. 26th ICRC, Salt Lake City, 3, 167
Apanasenko, A. V., et al. (RUNJOB collaboration) 1999c, Proc. 26th ICRC, Salt Lake City, 3, 235
Apanasenko, A. V., et al. (RUNJOB collaboration) 2000, preprint ICRR-Report-459-2000-3
Apanasenko, A. V., et al. (RUNJOB collaboration) 2001, Astropart. Phys., 16, 13
Asakimori, K. 1998, ApJ, 502, 278
Atkins, R., et al. 2005, [arXiv:astro-ph/0502303]
Berezovskaya, V. A., et al. 1997, Proc. 25th ICRC, Durban, South Africa, 6, 133
Biller, S., & Buckley, J. 1998, Phys. Rev. D, 57, 2637
Burnett, T., Dake, S., Derrickson, J., et al. 1990, ApJ, 349, L25
Fuki, M. 2001, http://akebono.ei.kochi-u.ac.jp/fuki/JACS/UTIL/CHAMBR/chamber.html
Hunter, S. D., Bertsch, D. L., Catelli, J. R., et al. 1997, ApJ, 481, 205
Kamioka, E., Hareyama, M., Ichimura, M., et al. 1997, Astropart. Phys., 6, 155
Kawamura, Y., Matsutani, H., Nanjyo, H., et al. 1989, Phys. Rev. D, 40, 729
Kobayakawa, K., et al. 2002, Phys. Rev. D, 66
Kopenkin, V., et al. 2002, Phys. Rev. D, 65, 072004
Kopenkin, V., et al. 2003, Phys. Rev. D, 68, 052007
Kopenkin, V., & Fujimoto, Y. 2005, Phys. Rev. D, 71, 023001
Nishimura, J., Fujii, M., Taira, T., et al. 1980, ApJ, 238, 394
Nishimura, J., et al. 1987, in Proceedings of Balloon Symposium, ed. J. Nishimura (Tokyo, Japan), 162
Ohishi, M., et al. 2005, Proc. 29th ICRC, Pune, India, 101
Perkins, D. H., & Fowler, P. H. 1964, Proc. Roy. Soc. A, 278, 401
Prouza, M., & Smida, K. 2003, A&A, 410, 1
RUNJOB collaboration 2000, Report on Japanese-Russian collaboration balloon experiment in 1996–1999, 08404012, (Study chief – H. Nanjo), Hirosaki University, 296
Seo, E. S. 2006, XIV ISVHECRI, Weihai, China, http://isvhecri2006.ihep.ac.cn/isvhecri2006/login.py?action=timetable
Shibata, T. 1999, Nucl. Phys. B, 75, 22
Strausz, S. C. 1997, Phys. Rev. D, 55, 4566
Takahashi, Y., et al. (JACEE collaboration) 1995, Proc. 24th ICRC, Rome, 2, 451
Takahashi, Y., Asakimori, K., et al. (JACEE collaboration) 1998, Nucl. Phys. B, 60, 83
Wefel, J. P., et al. (ATIC collaboration) 2005, Proc. 29th ICRC, Pune, India, 3, 105
Wiebel-Sooth, B., et al. 1988, A&A, 330, 389
Zatsepin, V. I. 1994, Proc. 23rd ICRC, Calgary, Canada, 5, 439